CELLULAR NEURAL NETWORKS: MOSAIC PATTERN AND SPATIAL CHAOS*

JONQ JUANG† AND SONG-SUN LIN†

Abstract. We consider a cellular neural network (CNN) with a bias term z in the integer lattice $\mathbf{Z}^2$ on the plane $\mathbf{R}^2$. We impose a symmetric coupling between nearest neighbors, and also between next-nearest neighbors. Two parameters, a and ε, are used to describe the weights between such interacting cells. We study patterns that can exist as stable equilibria. In particular, the relationship between mosaic patterns and the parameter space $(z, a; \varepsilon)$ can be completely characterized. This, in turn, addresses the so-called learning problem in CNNs. The complexities of mosaic patterns are also addressed.

Key words. cellular neural networks, pattern formation, spatial chaos

AMS subject classifications. Primary, 34C35; Secondary, 94C99

PII. S0036139997323607

1. Introduction. Many systems have been studied as models for spatial pattern formation in biology, chemistry, and physics. The types of systems we are interested in are large arrays of locally coupled first-order nonlinear dynamical systems, namely, cellular neural networks (CNNs). Such a class of information processing systems has been proposed by Chua and Young [12, 13]. The CNNs without input terms are of the form

$$(1.1a) \qquad \frac{dx_{i,j}}{dt} = -x_{i,j} + z + \sum_{|k|\leq 1, |\ell|\leq 1} a_{k,\ell} f(x_{i+k,j+\ell}), \ (i,j) \in \mathcal{Z}^2,$$

$$(1.1b) \qquad x_{i,j}(0) = x_{i,j}^0.$$

Here the nonlinearity f is a piecewise-linear function of the form

$$(1.2) \qquad f(x) = \frac{1}{2}(|x+1| - |x-1|).$$

The numbers $a_{k,\ell}$, $|k| \leq 1$, $|\ell| \leq 1$, $k, \ell \in \mathcal{Z}$, are arranged in a 3×3 matrix form, which is called a space-invariant A-template

$$(1.3) \qquad A = \begin{bmatrix} a_{-1,1} & a_{01} & a_{1,1} \\ a_{-1,0} & a_{0,0} & a_{1,0} \\ a_{-1,-1} & a_{0,-1} & a_{1,-1} \end{bmatrix}.$$

A is called symmetric if $a_{-k,-l} = a_{k,l}$ for all $|k| \leq 1$ and $|l| \leq 1$. The quantities $x_{i,j}$ denote the state of a cell $C_{i,j}$. If $x_{i,j} > 1$ (resp., $x_{i,j} < -1$), then its corresponding cell $C_{i,j}$ is called a positively (resp., negatively) saturated cell. If $|x_{i,j}| < 1$, then its associated cell $C_{i,j}$ is called a defect cell or a defect. The output of a cell $C_{i,j}$,

†Department of Applied Mathematics, National Chiao-Tung University, Hsinchu, Taiwan 31015, ROC (jjuang@math.nctu.edu.tw, sslin@math.nctu.edu.tw).

defined as $y_{i,j} = f(x_{i,j})$, is thus always bounded by $|y_{i,j}| \leq 1$. The quantity z is an independent voltage source. When $z = 0$, (1.1) is called unbiased; when $z \neq 0$, it is called biased.

Like a neural network, it is a large-scale nonlinear analog circuit which processes signals in real time. Like cellular automata, it is made of a massive aggregate of regularly spaced circuit clones called cells, which communicate with each other directly only through their nearest neighbors. Each cell is made of a linear capacitor, a nonlinear voltage-controlled current source, and a few resistive linear circuit elements. Such systems share the best features of neural networks and cellular automata; their continuous-time feature allows the real-time signal processing found wanting in the digital domain, and their local interconnection feature makes them ideal for very-large-scale-integrated (VLSI) implementation. Due to their local connectivity, CNNs can be realized as VLSI chips and can operate at a very high speed and complexity. Applications to image processing and pattern recognition can be found in [13]. Recently, the applicability of CNNs to important PDEs—autowaves and spiral waves in a reaction-diffusion-type system, Burger's equation, and the Navier–Stokes equation for incompressible fluids—is investigated in [36]. Moreover, since its invention in 1988, while retaining the two basic concepts of local connections and analog circuit dynamics, the CNN has evolved to cover a very broad class of problems and frameworks. For instance, it was found [39] that the CNN can produce patterns similar to those found in Ising spin glass systems, discrete bistable systems, and the reaction-diffusion system. For additional background information, applications, and theory, see [11, 12, 13, 16, 31, 34, 39] among others.

Lattices also play important, and in some cases essential, roles in many scientific models, typically modeling underlying spatial structures. We mention, in particular, models arising from chemical reactions [9, 29], biology [3, 4, 17, 18, 27, 30, 40], material science [5, 14, 22], and image-processing and pattern-recognition [11, 12, 13, 20, 39]. Much theoretical work in lattice differential equations concerns one-dimensional lattices. Some theoretical approaches to systems of higher dimensions have been made; see, e.g., [8, 9, 31]. Recent results on traveling and propagating waves can be found in [1, 2, 6, 7, 10, 19, 32, 33]. A special issue on nonlinear waves, patterns, and spatio-temporal chaos in dynamic arrays is reported in [41].

Stationary solutions $\bar{x} = (\bar{x}_{i,j})$ of (1.1a) are very important in studying CNN systems; their outputs $\bar{y} = (f(\bar{x}_{i,j}))$ are called patterns. Indeed, when people study the long-time behavior of any dynamical system, the stationary solutions are the basic and simplest objects that have to be considered. Usually, the existence of multiple stationary solutions may induce complicated phenomena of the dynamical system. In the case of CNNs, it was shown by Chua and Yang [12] that (1.1a) behavior is like a gradient system when template A is symmetric and the lattice is finite. In this case, every trajectory will tend to a stable stationary solution as time goes up. In an infinite system as (1.1a) with symmetric template, it is conjectured that most trajectories will end up at stable stationary solutions. However, a verification remains demanded. In this paper we study only stationary solutions; other types of solutions are studied elsewhere [24].

Two types of stationary solution are of interest: mosaic and defect. A mosaic solution $\bar{x}$ satisfies $|\bar{x}_{i,j}| > 1$ for all $(i,j) \in \mathcal{Z}^2$. A defect solution $\bar{x}$ satisfies $|\bar{x}_{i,j}| > 1$ for $(i,j) \in \mathcal{Z}^2 \backslash D$ and $|\bar{x}_{k,\ell}| < 1$ for $(k,\ell) \in D$, where $D \neq \phi$ and $D \neq \mathcal{Z}^2$. Their corresponding pattern $\bar{y}$ can thus be called a mosaic and a defect pattern, respectively.

One basic problem in CNN theory is the so-called learning problem, which can

be stated as follows:

(1.4a) Given a set of stationary patterns $\mathcal{U}$, determine a set of parameters $\mathcal{P} \subset \mathcal{P}_{10} = \{z, a_{k,\ell} : k, \ell \text{ integer and } |k|, |\ell| \leq 1\}$, and a parameter space, such that any pattern in $\mathcal{U}$ can be obtained and is stable for all parameters in $\mathcal{P}$.

The "learning problem" is almost the inverse of the following problem.

(1.4b) Given any $\mathcal{P} \subset \mathcal{P}_{10}$, determine $\mathcal{M}(\mathcal{P})$ (resp., $\mathcal{D}(\mathcal{P})$), the set of all stable mosaic (resp., defect) patterns of (1.1).

Furthermore, we also wish to address

(1.4c) the complexity of $\mathcal{M}(\mathcal{P})$ and $\mathcal{D}(\mathcal{P})$ for each subset $\mathcal{P}$ of $\mathcal{P}_{10}$.

To study these problems, we begin with a local solution y_T of (1.1a) which is defined on a certain subsets T of $\mathcal{Z}^2$. The associated output y_T is called a local pattern; for details see Definition 4.2. We find that the parameter space $\mathcal{P}_{10}$ can be partitioned finitely into many regions $\{\mathcal{P}^{(k)}\}_{k \in K}$. Only a few local patterns are stable in each region $\mathcal{P}^{(k)}$; these are called the feasible patterns of region $\mathcal{P}^{(k)}$. In principle, we can obtain all stable patterns by patching these feasible patterns together. However, to construct all stable patterns of $\mathcal{P}^{(k)}$ more efficiently, we introduce a set $B(\mathcal{P}^{(k)})$ of local patterns, so-called "building blocks" for each region $\mathcal{P}^{(k)}$; see Definition 4.6. Then, using certain compatibility rules $\mathcal{C}(\mathcal{P}^{(k)})$, we can patch these building blocks together into a global pattern in $\mathcal{Z}^2$. These building blocks and compatibility conditions also enable us to estimate the spatial entropy $h(\mathcal{M}(\mathcal{P}^{(k)}))$ and $h(\mathcal{D}(\mathcal{P}^{(k)}))$ of $\mathcal{M}(\mathcal{P}^{(k)})$ and $\mathcal{D}(\mathcal{P}^{(k)})$, the set of all mosaic patterns and defect patterns, respectively.

For simplicity, in this paper we emphasis the case in which template A is a square cross, e.g.,

$$(1.5) \qquad\qquad A = \left[\begin{array}{ccc} 0 & b & 0 \\ b & a & b \\ 0 & b & 0 \end{array} \right].$$

For this case, we completely solve the problems in (1.4) for the set of stable mosaic patterns. The method is quite general and can be applied to more general templates A [25] and to study the set of stable defect patterns [26].

We remark that there are many numerical computation results which have been obtained, especially in papers published in the *IEEE Transactions on Circuits and Systems*, since 1988 [11, 12, 13, 15, 16, 19, 33, 36, 39, 41]. Furthermore, people can now do some numerical experiments through the World Wide Web; see [21]. One will find some interesting phenomena on a 20×20 square lattice by changing various parameters and using different initial data. It is clear that all numerical results are based on the model on finite lattices [6, 7, 8, 9, 10, 23, 24, 25, 26, 27, 28, 32, 33, 37, 38, 39]. The mathematical theory developed in this paper and many others is based on infinite lattices. Therefore, it is important to know the relationships between infinite lattices and large but finite lattices, especially the problem of influence of boundary conditions on finite lattices. In the case of one-dimensional CNNs, there is an affirmative result recently obtained by Shih [38]. Indeed, he proved that the limiting spatial entropies are equal for periodic, Dirichlet, and Neumann boundary conditions as the size of lattices tend to infinite, i.e., the impact of boundary conditions is very weak in a one-dimensional case. As for two-dimensional CNNs the problem is still unsettled. In general, the problem of lattice dynamical systems between infinite size and finite but large size is still wide open and challenging.

We conclude this introductory section by summarizing the organization of this paper. In section 2, we discuss the (linearized) stability of stationary solutions and

then review some basic results concerning spatial entropy. In section 3, we introduce a geometrical method for partitioning the parameter space into finite many disjoint regions. In section 4, we give a complete classification of the set of mosaic patterns in each region. The lower spatial entropy bound of these sets of mosaic patterns is also computed. The results concerning the mosaic patterns for a one-dimensional CNN system is recorded in section 5.

2. Pattern and spatial entropy. Given template A and a biased term z, the stationary (steady-state, equilibrium) equation for (1.1a) is

$$(2.1) \qquad x_{i,j} = z + \sum_{|k|\leq 1,|\ell|\leq 1} a_{k,\ell} f(x_{i+k,j+\ell}), (i,j) \in \mathcal{Z}^2.$$

Let $x = (x_{i,j})$ be a solution of (2.1). The associated output $y = (y_{i,j}) = (f(x_{i,j}))$ is called a (stationary) pattern. These stationary solutions can be classified into four types.

DEFINITION 2.1. *A solution* $x = (x_{i,j})$ *of* (2.1) *is called nontransitional if* $|x_{i,j}| \neq 1$ *for all* $(i,j) \in \mathcal{Z}^2$. *In particular,* x *is called a mosaic solution if* $|x_{i,j}| > 1$ *for all* $(i,j) \in \mathcal{Z}^2$. *Its associated pattern is called a mosaic pattern. If* $|x_{i,j}| < 1$ *for all* $(i,j) \in \mathcal{Z}^2$, *then* x *and* $y = (f(x_{i,j}))$ *are called, respectively, an interior solution and an interior pattern. If* $|x_{i,j}| \neq 1$ *for all* $(i,j) \in \mathcal{Z}^2$ *and there are* (m,n) *and* (k,ℓ) *such that* $|x_{m,n}| < 1$ *and* $|x_{k,\ell}| > 1$, *then* x *and* $y = (f(x_{i,j}))$ *are called, respectively, a defect solution and a defect pattern. If there exists an* (i,j) *such that* $|x_{ij}| = 1$, *then* x *and* $y = (f(x_{i,j}))$ *are called, respectively, a transition solution and a transition pattern.*

Given a nontransitional solution $x = (x_{i,j})$ of (2.1), we denote Γ_+, Γ_-, and $\Gamma_\times$ as

$$(2.2a) \qquad \Gamma_+ = \{(i,j) \in \mathcal{Z}^2 : x_{i,j} > 1\},$$

$$(2.2b) \qquad \Gamma_- = \{(i,j) \in \mathcal{Z}^2 : x_{i,j} < -1\},$$

and

$$(2.2c) \qquad \Gamma_\times = \{(i,j) \in \mathcal{Z}^2 : |x_{i,j}| < 1\},$$

respectively. Stability is then studied using spectral theory. Let $\xi = (\xi_{i,j}) \in \ell^2$. The linearized operator $\mathcal{L}(x)$ of (2.1) at x is given by

$$(2.3a,b) \qquad (\mathcal{L}(x)\xi)_{i,j} = \begin{cases} -\xi_{i,j} + L_{i,j} & \text{if } (i,j) \in \Gamma_+ \cup \Gamma_-, \\ (a_{0,0}-1)\xi_{i,j} + L_{i,j} & \text{if } (i,j) \in \Gamma_\times. \end{cases}$$

Here,

$$(2.3c) \qquad L_{i,j} = \sum_{(k,\ell)\in N^+,(i,j)\cap\Gamma_\times} a_{k-i,\ell-j}\xi_{k,\ell}$$

and

$$(2.3d) \qquad N^+(i,j) = \{(p,q) \in \mathcal{Z}^2 : |p-i| + |q-j| = 1\}.$$

DEFINITION 2.2. *Let* x *be a solution of* (2.1) *with* $|x_{i,j}| \neq 1$ *for all* $(i,j) \in \mathcal{Z}^2$. x *is then called (linearized) stable if all eigenvalues of* $\mathcal{L}(x)$ *have negative real parts.*

The solution x is called unstable if there is an eigenvalue λ of $\mathcal{L}(x)$ such that λ has a positive real part.

DEFINITION 2.3. *A solution $x = (x_{i,j})$ of* (2.1) *is said to be feasible provided that it is stable.*

We then have the following stability result.

THEOREM 2.4. *Let $x = (x_{i,j})$ be a solution of* (2.1). *The following holds.*

(i) *If x is a mosaic solution, then x is stable. Hence, for a mosaic solution, existence implies feasibility.*

(ii) *If $a_{0,0} > 1$, and x is an interior or a defect solution, then x is unstable.*

Proof. If x is a mosaic solution, then $-\mathcal{L}(x)$ is a self-adjoint and positive operator. The first assertion of the theorem thus follows. Next, let x be an interior or a defect solution. Let $\tilde{\ell}^2 = \{\zeta = (\zeta_{ij}) \in \ell^2 : \zeta_{ij} = 0 \text{ for all } (i,j) \in \Gamma_+ \cup \Gamma_-.\}$. Then $\mathcal{L}(x)|_{\tilde{\ell}^2} : \tilde{\ell}^2 \to \tilde{\ell}^2$ is also a self-adjoint operator. Moreover, if λ is an eigenvalue of $\mathcal{L}(x)|_{\tilde{\ell}^2}$, then λ is also an eigenvalue of $\mathcal{L}(x)$. Hence, in completing the proof, it suffices to show that $-\mathcal{L}(x)|_{\tilde{\ell}^2}$ is not a positive operator when $a_{0,0} > 1$. To this end, let $(i_0, j_0) \in \Gamma_\times$ and let $e = (e_{i,j})$ be such that

$$e_{i,j} = \begin{cases} 1 & (i,j) = (i_0, j_0), \\ 0 & \text{otherwise.} \end{cases}$$

Then,

$$\langle -\mathcal{L}(x)e, e \rangle = 1 - a_{0,0} < 0.$$

This completes the proof of Theorem 2.4. □

For completeness we review some definitions and results concerning spatial entropy. For more details see [8, 35].

Let $\mathcal{A}$ be a finite set of D elements (an alphabet) and $D \geq 1$ be an integer (the lattice dimension). Denote by $\mathcal{A}^{\mathcal{Z}^D}$ the set of all $y : \mathcal{Z}^D \to \mathcal{A}$. In our case, $D = 2$ and $\mathcal{A} = \{-1, 1\}$ for the mosaic patterns.

DEFINITION 2.5. *Let $\mathcal{U}$ be a translation-invariant subset of $\mathcal{A}^{\mathcal{Z}^D}$; $\mathcal{U}$ is called spatial chaos if the spatial entropy $h(\mathcal{U})$ (see* [10, 39]) *is greater than zero. Otherwise, $\mathcal{U}$ is called pattern formation.*

3. Partitioning the parameter spaces. Let template A be square-crossed, e.g.,

$$(3.1) \qquad A = A^+ \equiv \begin{bmatrix} 0 & b & 0 \\ b & a & b \\ 0 & b & 0 \end{bmatrix} \quad \text{or} \quad \begin{bmatrix} 0 & a\varepsilon & 0 \\ a\varepsilon & a & a\varepsilon \\ 0 & a\varepsilon & 0 \end{bmatrix},$$

where $a\varepsilon = b$ if $a \neq 0$. We then have three parameters, $a, b,$ and z or $a, \varepsilon,$ and z. In this section, we shall partition the parameter spaces $\mathcal{P}_3 = \{(z, a, b) : a, b, z \in \mathcal{R}\}$ or $= \{(z, a, \varepsilon) : a, \varepsilon, z \in \mathcal{R}\}$ into finitely many regions such that in each region, (2.1) has the same mosaic patterns.

From now on, we shall assume that (3.1) holds. When $a \neq 0$ and x is a solution, then for any $(i, j) \in \mathcal{Z}^2, (x_{i,j}, y_{i,j})$ will satisfy

$$(3.2) \qquad y = f(x)$$

and

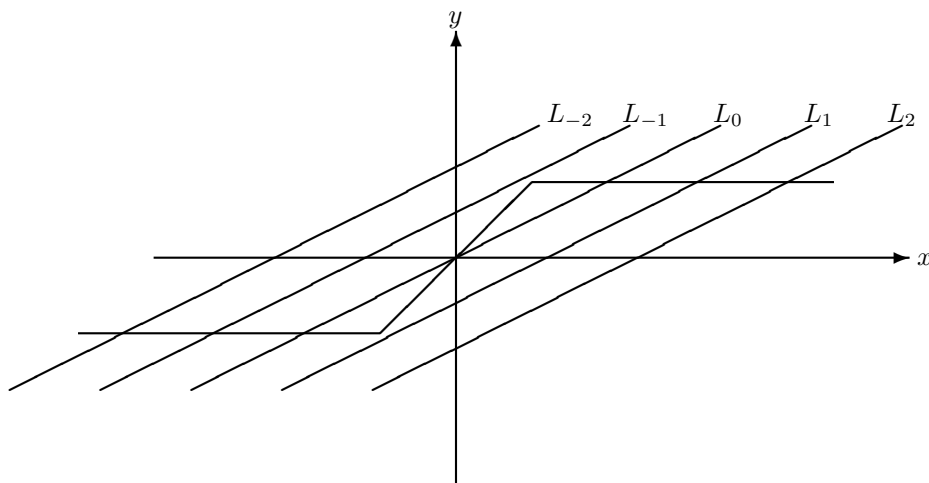$$(3.3a) \qquad y = \frac{1}{a}\{x - (z + 2kb)\},$$

FIG. 3.1. $a > 0$, $\varepsilon > 0$, $m = 3 = n$. Here $L_i = L_{i,\varepsilon}$, $i \in I[-2, 2]$.

or

(3.3b)
$$y = \frac{1}{a}\{x - (z + 2ka\varepsilon)\},$$

for $k \in \{-2, -1, 0, 1, 2\}$, i.e., $(x_{i,j}, f(x_{i,j}))$ lies on one of the five straight lines $L_{k,\varepsilon}$ defined in (3.3), where z, a, and b are fixed; see Figures 3.1 and 3.2. For $a = 0$, (3.3) reduces to

(3.3c)
$$x - z - 2kb = 0.$$

Note that when $k = 2$, this corresponds to an unknown cell $C_{i,j}$ being surrounded by four positively saturated cells. Similar interpretations can be applied to $k = 1, 0, -1, -2$. If the dependence of the solutions of (3.2) and (3.3) on k is emphasized, we shall denote the solutions by $x(k)$. Clearly, $x(k)$ is strictly monotonous in k provided that $b \neq 0$. Such monotonicity plays a crucial role in grouping the parameters in $\mathcal{P}_3$ so that the questions in (1.4a) and (1.4b) can be completely answered.

To pursue this idea for partitioning $\mathcal{P}_3$ in more detail, we first need the following notation.

DEFINITION 3.1. *For any two integers $k < \ell$, denote $I[k, \ell] = \{k, k + 1, \ldots, \ell\}$, the set of integers that are no greater than ℓ and no smaller than k.*

DEFINITION 3.2. *For $m, n \in I[0, 5]$, denote $[m, n]$ the (open) subset of $\mathcal{P}_3$ such that the intersection of (3.2) and (3.3) consists of m positively saturated states; i.e., $(x > 1)$ and there are n negatively saturated states (i.e., $(x < -1)$). Furthermore, for any fixed b or ε, we may also use $[m, n]$, or $[m, n]_b$ or $[m, n]_\varepsilon$ if necessary, to describe such an open subset in $\mathcal{P}_2 = \{(z, a) : z, a \in \mathcal{R}\}$.*

To clarify Definition 3.2, we give Figure 3.1 with various m and n.

It is much easier to partition $\mathcal{P}_2$ into $[m, n]_\varepsilon$ by fixing and then varying $\varepsilon \in \mathcal{R}$. Indeed, for each ε and $k \in I[-2, 2]$, let $r_{k,\varepsilon}$ and $\ell_{k,\varepsilon}$ be straight lines whose equations are

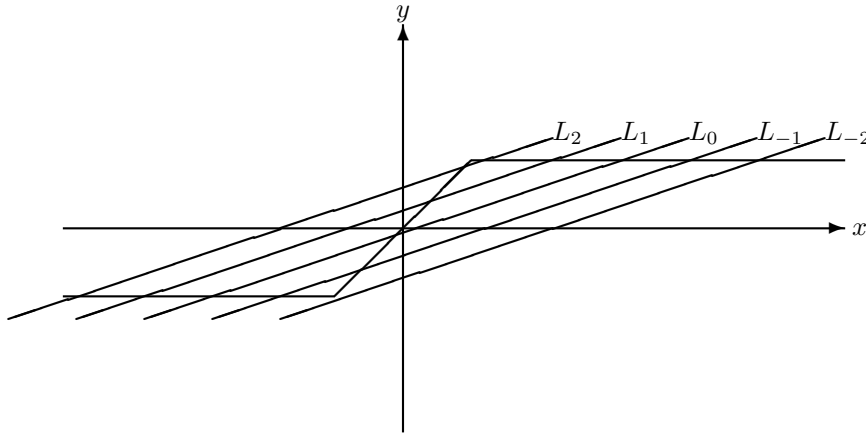(3.4a)
$$r_{k,\varepsilon} : z + (1 + 2k\varepsilon)a = 1$$

FIG. 3.2. $a > 0$, $\varepsilon < 0$, $m = 5$, $n = 4$.

and

(3.4b) $$\ell_{k,\varepsilon} : -z + (1 - 2k\varepsilon)a = 1.$$

Note that $r_{k,\varepsilon}$ and $\ell_{k,\varepsilon}$ are projections of the planes r_k and ℓ_k in $\mathcal{P}_3$ obtained by defining

(3.5) $$r_k : a + z + 2kb = 1$$

and

(3.6) $$\ell_k : a - (z + 2kb) = 1,$$

which, in turn, are obtained by respective substitutions of $(x, y) = (1, 1)$ and $(x, y) = (-1, -1)$ into (3,4). We will see later that lines $\{r_{k,\varepsilon}, \ell_{k,\varepsilon}\}_{k \in I[-2,2]}$ cut $\mathcal{P}_2$ into disjoint regions $[m, n]_\varepsilon$, $m, n \in I[0, 5]$, as do the planes $\{r_k, \ell_k\}_{k \in I[-2,2]}$ in $\mathcal{P}_3$.

DEFINITION 3.3. *Let ℓ be a straight line that does not pass through the origin in $\mathcal{P}_2$. Denote by $\ell(0)$ the open half-plane containing the origin, while $\ell(\times)$ denotes the other open half-plane. Furthermore, for any ε and $k \in I[-2, 2]$, denote*

(3.7a) $$P_{k,\varepsilon} \equiv r_{k,\varepsilon}(\times) \cap \ell_{k,\varepsilon}(0),$$
(3.7b) $$M_{k,\varepsilon} \equiv r_{k,\varepsilon}(\times) \cap \ell_{k,\varepsilon}(\times),$$
(3.7c) $$N_{k,\varepsilon} \equiv r_{k,\varepsilon}(0) \cap \ell_{k,\varepsilon}(\times),$$
(3.7d) $$I_{k,\varepsilon} \equiv r_{k,\varepsilon}(0) \cap \ell_{k,\varepsilon}(0).$$

We then have the following result.

PROPOSITION 3.4. *Given $k \in I[-2, 2]$ and $\varepsilon \neq 0$, if $(z, a) \in \mathcal{P}_{k,\varepsilon}$, then the straight line $L_{k,\varepsilon}$ defined by (3.3) intersects the graph of (3.2) only in a positively saturated state (e.g., $x > 1$). Similarly, if (z, a) is in $N_{k,\varepsilon}, M_{k,\varepsilon}$, and $I_{k,\varepsilon}$, resp., then $L_{k,\varepsilon}$ intersects (3.2) only in a negatively saturated state (e.g., $x < -1$), positively and negatively saturated states (e.g., $|x| > 1$), or only in a defect state (e.g., $|x| < 1$).*

The proof of this proposition is elementary but lengthy, so we omit it. An illustration of regions for $k = 2$ and $\varepsilon = \frac{1}{8}$ is given in Figure 3.3.
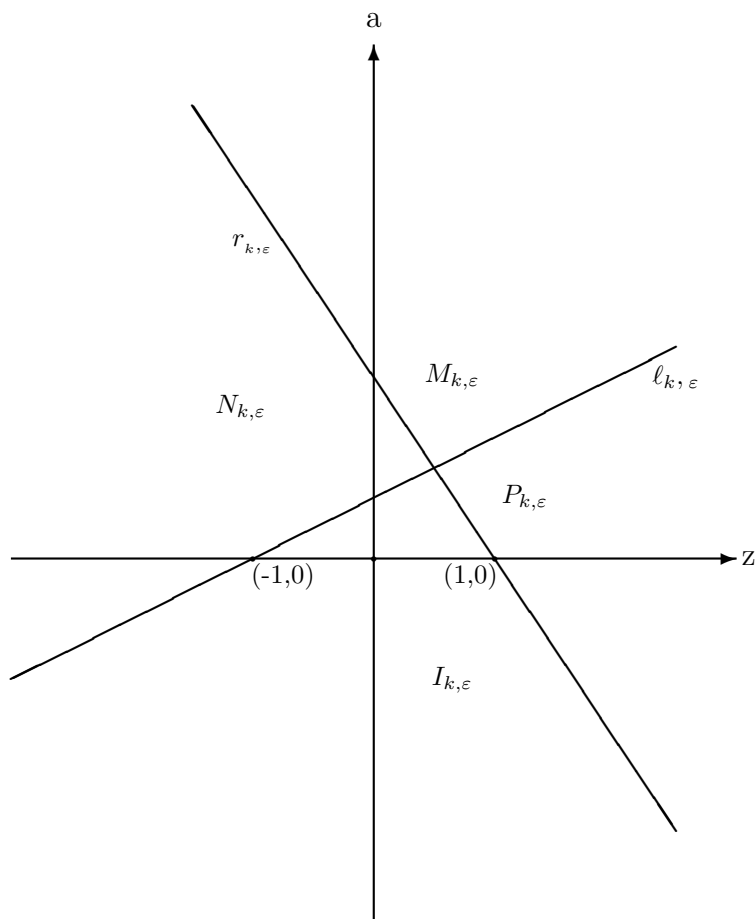
FIG. 3.3. $k = 2$, $\varepsilon = -\frac{1}{8}$.

We now can state our main result concerning the partitioning of $\mathcal{P}_2$ by $[m, n]_\varepsilon$.

THEOREM 3.5. *Let $\mathcal{P}_2^+$ and $\mathcal{P}_2^-$ be the open upper half-plane and lower half-plane, respectively. Then the following results hold:*

(I) *For $0 < |\varepsilon| < \frac{1}{4}$, and any $m, n \in I[0,5]$, we have*

$$(3.8) \qquad [m, n]_\varepsilon = r_{2-m, |\varepsilon|}(0) \cap r_{3-m, |\varepsilon|}(\times) \cap \ell_{n-2, |\varepsilon|}(0) \cap \ell_{n-3, |\varepsilon|}(\times).$$

Here, if $|k| > 2$, then $r_{k, |\varepsilon|}(\cdot)$ is interpreted as $\mathcal{P}_2$. Furthermore, $\mathcal{P}_2^+$ is the union of those mutually disjoint sets $[m, n]_\varepsilon$ and their boundaries, e.g.,

$$(3.9) \qquad \overline{\mathcal{P}_2^+} = \bigcup_{m, n \in I[0,5]} \overline{[m, n]_\varepsilon \cap \mathcal{P}_2^+}.$$

Here, $\overline{S}$ is the closure of set S in $\mathcal{P}_2$. Similarly, we have

$$(3.10) \qquad \overline{\mathcal{P}_2^-} = \bigcup_{\substack{m, n \in I[0,5] \\ m \cdot n = 0}} \overline{[m, n]_\varepsilon \cap \mathcal{P}_2^-}.$$

Here, for $m, n \in I[1, 5]$,

$$(3.11) \qquad\qquad [m, 0]_\varepsilon = r_{m-2,|\varepsilon|}(0) \cap r_{m-3,|\varepsilon|}(\times),$$

$$(3.12) \qquad\qquad [0, n]_\varepsilon = \ell_{2-n,|\varepsilon|}(0) \cap \ell_{3-n,|\varepsilon|}(\times),$$

and

$$(3.13) \qquad\qquad [0, 0]_\varepsilon = r_{-2,|\varepsilon|}(0) \cap \ell_{2,|\varepsilon|}(0).$$

A decomposition of $\mathcal{P}_2$ in terms of $[m, n]_\varepsilon$ is given in Figure 3.4.
  (II) *For $\frac{1}{4} \leq |\varepsilon| < \frac{1}{2}$, similar conclusions as those in* (I) *hold except that*
    (i) $[5, 5]_\varepsilon = \phi$,
    (ii) *for $\frac{1}{4} < |\varepsilon| < \frac{1}{2}$,*

$$[1, 0]_\varepsilon \cap \mathcal{P}_2^- = r_{-1,|\varepsilon|}(0) \cap r_{-2,|\varepsilon|}(\times) \cap \ell_{2,|\varepsilon|}(0) \cap \mathcal{P}_2^-,$$
$$[0, 1]_\varepsilon \cap \mathcal{P}_2^- = r_{-2,|\varepsilon|}(0) \cap \ell_{-1,|\varepsilon|}(0) \cap \ell_{2,|\varepsilon|}(\times) \cap \mathcal{P}_2^-,$$
$$[0, 0]_\varepsilon \cap \mathcal{P}_2^- = r_{-2,|\varepsilon|}(\times) \cap \ell_{2,\varepsilon}(\times) \cap \mathcal{P}_2^-.$$

See Figure 3.5.
  (III) *For $\varepsilon = \frac{1}{2}$, we have*

$$\overline{\mathcal{P}_2^+} = \bigcup_{\substack{m,n \in I[0,5] \\ m+n \leq 7}} \overline{[m, n]_\varepsilon \cap \mathcal{P}_2^+}$$

and $\mathcal{P}_2^- \cap [m, n] \neq \phi$, if and only if $m, n \in I[0, 5]$ and $m + n < 4$.
  (IV) *For $\frac{1}{2} < |\varepsilon| < 1$, we have $\mathcal{P}_2^+$, as in* (III), *and*

$$\mathcal{P}_2^- \cap [m, n]_\varepsilon \neq \phi,$$

if and only if $m, n \in I[0, 5]$ and $m + n < 5$. See Figure 3.6.

  (V) *For $|\varepsilon| = 1$, we have*

$$\overline{\mathcal{P}_2^+} = \bigcup_{\substack{m,n \in I[0,5] \\ m+n \leq 6}} \overline{[m, n]_\varepsilon \cap \mathcal{P}_2^+}$$

and $\mathcal{P}_2^-$ is as in (IV).

  (VI) *For $|\varepsilon| > 1$, we have $\mathcal{P}_2^+$ as in* (V) *and*

$$\mathcal{P}_2^- \cap [m, n]_\varepsilon \neq \phi,$$

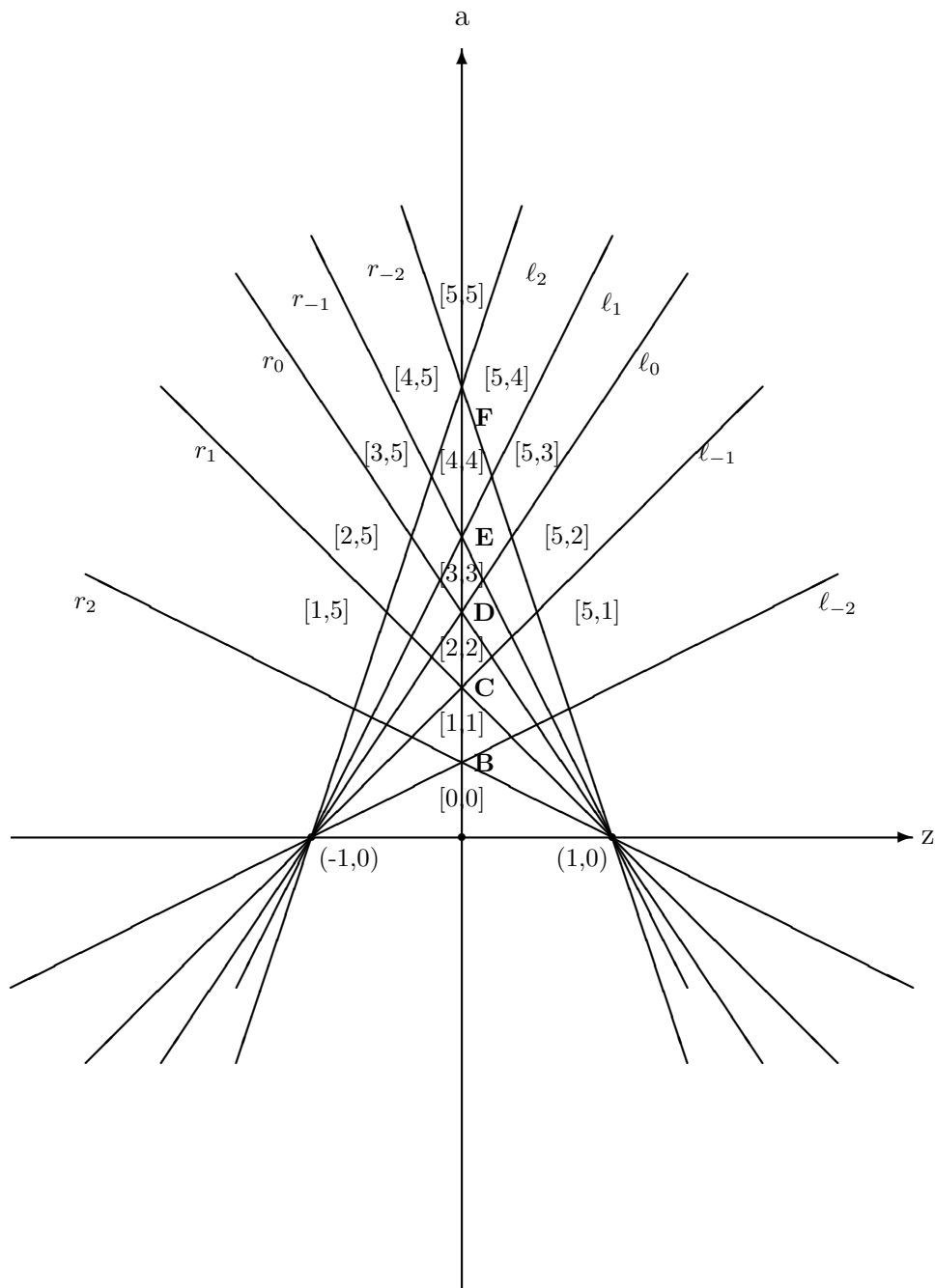*if and only if $m, n \in I[0, 5]$ and $m + n < 6$. See Figure 3.7.*

FIG. 3.4. $B = \frac{1}{1+4|\varepsilon|}$, $C = \frac{1}{1+2|\varepsilon|}$, $D = 1$, $E = \frac{1}{1-2|\varepsilon|}$, $F = \frac{1}{1-4|\varepsilon|}$, $0 < |\varepsilon| < \frac{1}{4}$.
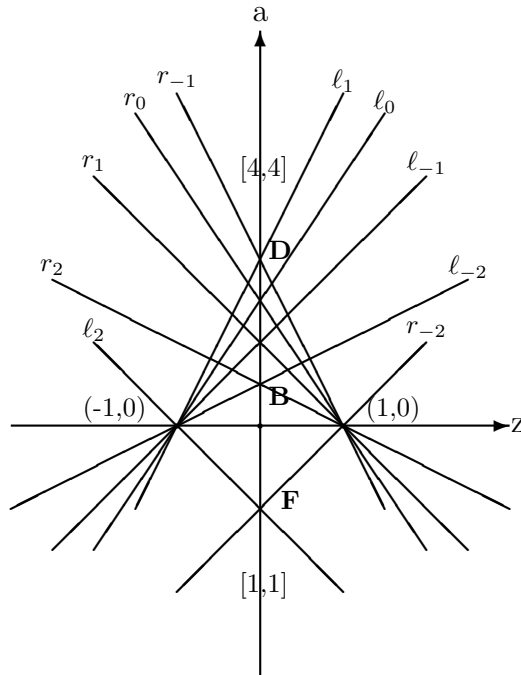
FIG. 3.5.

To conserve the notation in Figures 3.3–3.6, we set $\ell_{i,\varepsilon} = \ell_i$, and $r_{i,\varepsilon} = r_i$, where $i \in I[1,5]$.

   Proof. To demonstrate the validity of the assertion in (3.8), we illustrate only how to compute $[3,3]_\varepsilon$. The other cases are obtained in similar fashion. For $a > 0$ and $\varepsilon > 0$, to have the intersections of (3.2) and (3.3b) contain three positively saturated states and three negatively saturated states, it is necessary and sufficient (see Figure 3.3) to have the parameters (z,a) lie in

$$N_{-1,\varepsilon} \cap M_{0,\varepsilon} \cap P_{1,\varepsilon}.$$

Using Proposition 3.4, we conclude that $[3,3]_\varepsilon$ should be as asserted. On the other hand, for $a > 0$ and $\varepsilon < 0$, to have $(z,a) \in [3,3]_\varepsilon$, it must be that (z,a) lies in

$$N_{1,\varepsilon} \cap M_{0,\varepsilon} \cap P_{-1,\varepsilon}.$$

Since $N_{1,\varepsilon} = N_{-1,-\varepsilon}, M_{0,\varepsilon} = M_{0,-\varepsilon}$, and $P_{-1,\varepsilon} = P_{1,-\varepsilon}$, we see that

$$[3,3]_\varepsilon = [3,3]_{-\varepsilon}.$$

The results for $[m,n]_\varepsilon$ in $\mathcal{P}^+$ can be verified in a similar fashion.

   Next we consider the region $[m,n]_\varepsilon$ contained in $\mathcal{P}_2^-$. Note that for $a < 0$, i.e., the slopes of the straight lines in (3.3b) are negative, it is impossible for the number of intersection points of (3.2) and (3.3b) to be greater than 5. Therefore,

$$[m,n]_\varepsilon \cap \mathcal{P}^- = \phi \quad \text{for all} \quad m+n \geq 6, m,n \in I[0,5].$$

Considering the region $\mathcal{P}^- \cap [3,1]_\varepsilon$, where $\varepsilon > 0$, we have

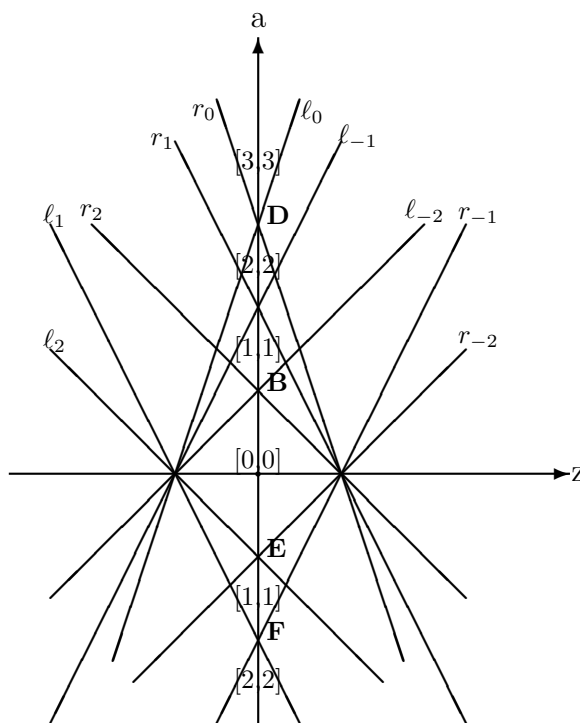$$\mathcal{P}^- \cap [3,1]_\varepsilon = P_{0,|\varepsilon|} \cap M_{1,|\varepsilon|} \cap N_{2,|\varepsilon|}.$$

Fig. 3.6.

Using Proposition 3.4, we get that

$$\mathcal{P}^- \cap [3,1]_\varepsilon \neq \phi \ \text{ if and only if } \ |\varepsilon| > \frac{1}{2}.$$

Proof of the remaining parts of the theorem is omitted.   □

Remark 3.6.

(i) The regions $[m,n]_\varepsilon$ and $[n,m]_\varepsilon$ are symmetric with respect to the a-axis.

(ii) Dependence of $[m,n]_\varepsilon$ on ε makes perfect sense. As $|\varepsilon|$ grows larger, the distances between the x-intercepts of the straight lines in (3.3) become larger. Consequently, for a fixed $a \neq 0$, as $|\varepsilon|$ increases, the number of straight lines in (3.3) that hit $y = f(x)$ at two different states or more will decrease; see Figures 3.1 and 3.2. Moreover, for $a < 0$, each of the straight lines in (3.3) cannot hit $y = f(x)$ more than once. Therefore, the region $[m,n]$, in which $m,n \geq 3$, cannot appear in the lower half-plane of P_2. Furthermore, for $a > 0$, as $|\varepsilon|$ becomes sufficiently large, only $L_{0,\varepsilon}$ can intersect $y = f(x)$ more than once. This explains why regions $[m,n]$, in which $m,n \geq 3$, and either $m > 3$ or $n > 3$, will gradually disappear as $|\varepsilon|$ grows.

Remark 3.7. Theorem 3.5 holds for the template

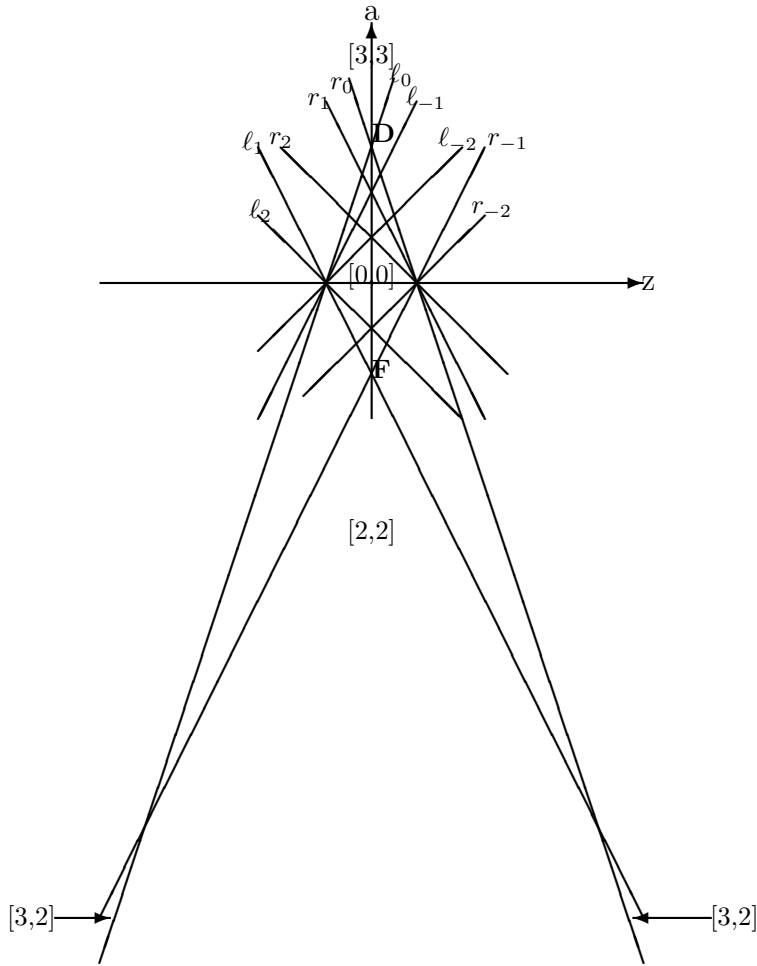$$(3.14a) \qquad\qquad A = \begin{bmatrix} 0 & \pm b & 0 \\ \pm b & a & \pm b \\ 0 & \pm b & 0 \end{bmatrix},$$

FIG. 3.7.

as well as

(3.14b)
$$A = \begin{bmatrix} \pm b & 0 & \pm b \\ 0 & a & 0 \\ \pm b & 0 & \pm b \end{bmatrix},$$

the diagonal-cross.

Remark 3.8. The idea of using (hyper-) planes to divide the parameter space into disjoint regions can be applied to any general template; see [25].

4. Mosaic solutions. In this section, we try to construct all mosaic patterns for each $[m, n]$ and, consequently, show that $[m, n]$ completely determines mosaic patterns. For each $[m, n]$, we begin with the study of feasible local patterns (see Definition 4.2). Using these feasible patterns, we can form a set of building blocks that can be glued together according to certain rules (compatibility conditions) to construct all mosaic patterns.

Next we introduce notation that describes the set of nearest neighbors, and the

set of next-nearest neighbors, to the point (i, j).

$$(4.1) \qquad N^+(i,j) = \{(i+k, j+\ell) \in \mathbf{Z}^2 : |k| + |\ell| = 1\},$$

$$(4.2) \qquad N^\times(i,j) = \{(i+k, j+\ell) \in \mathbf{Z}^2 : |k| + |\ell| = 2\}.$$

Below, we consider cells coupled (attached) to each other if and only if they are vertically or horizontally adjacent to each other. Since N^+ and $N^\times$ have symmetric properties, e.g., $(k, \ell) \in N^+(i,j)$ (or $N^\times(i,j)$) if and only if $(i,j) \in N^+(k, \ell)$ (or $N^\times(k, \ell)$), a cell $C_{k,\ell}$ is coupled (attached) to a cell $C_{i,j}$ if and only if $(k, \ell) \in N^+(i,j)$, and vice versa. Accordingly, we say two states or two patterns (outputs) are coupled to each other if their associated cells are coupled to each other. We have the basic result for $[m,n]_\varepsilon$ as follows.

LEMMA 4.1 (existence or feasibility lemma for $[m, n]_\varepsilon$). *Given parameters z, a, and ε in $[m,n]_\varepsilon$, and that $a\varepsilon > 0$, $x = (x_{ij})$ is a (feasible) solution if and only if any positively (resp., negatively) saturated cells must be coupled to at least $5 - m$ positively (resp., $5 - n$ negatively) saturated cells. On the other hand, if $a\varepsilon < 0$, then any positively (resp., negatively) saturated cell must be coupled to at least $5 - m$ negatively (resp., $5 - n$ positively) saturated cells.*

The proof of the lemma follows easily from Proposition 3.4, Theorems 3.5 and 2.4, and Definition 3.2, and so is omitted here.

Note that the constraints given in Lemma 4.1 are basic, and also that only these constraints must be obeyed in obtaining a global pattern. Next we introduce the following feasibility conditions for local patterns for which we need the following notation.

DEFINITION 4.2. *Given any (proper) subset $T \subseteq \mathcal{Z}^2$, $x(\equiv x_T)$ is called a local solution if x_T is a restriction of some mosaic solution x of (2.1) on T. Similarly, $y(\equiv y_T) : T \to \{-1, 1\}$ is called a local pattern if it is an output of some (local) solution x of (2.1) on T. When $T = \mathcal{Z}^2$, y is called a global pattern. A set $T \subseteq \mathcal{Z}^2$ is called basic with respect to the template A if $T = T_{i,j} \equiv \{(i,j)\} \cup N^+(i,j)$ for some $(i, j) \in \mathcal{Z}^2$. A basic pattern (BP) y is a feasible pattern defined on some basic set. Denote by $\mathcal{F}([m, n])$ the set of all feasible basic patterns that have parameters in $[m, n]$.*

Since our template A is spatially-invariant, (2.1) is then translation-invariant over $\mathcal{Z}^2$. Two sets T_1 and T_2 in $\mathcal{Z}^2$ are translation-invariant if $T_2 = T_1 + (k, \ell)$ for some (k, ℓ). Therefore, two local patterns y_{T_1} and y_{T_2} are (translation) equivalent if T_1 and T_2 are translation-invariant, and $(y_{T_2})_{i+k, j+\ell} = (y_{T_1})_{i,j}$ for any $(i, j) \in T_1$. We will distinguish between equivalent patterns only to eliminate any possibility of confusion.

An easy consequence of Lemma 4.1 is the following assertion.

PROPOSITION 4.3. *For any $[m, n]$, $\mathcal{F}([m, n])$ is unique and finite.*

We now give a partial list of possible $\mathcal{F}([m, n])$.

DEFINITION 4.4. *Given a set of (local or global) patterns $Y = \{y_\alpha\}$, we denote by $R(Y)$ the set of all patterns that are rotated by multiples of $90°$ from original patterns in Y.*

EXAMPLE 4.5. *Suppose $a\varepsilon > 0$; let $\bullet$ be either $+$ or $-$. Then*

(i) $\mathcal{F}([5,5]) = \left\{ \begin{smallmatrix} & \bullet & \\ \bullet & + & \bullet \\ & \bullet & \end{smallmatrix} \,, \begin{smallmatrix} & \bullet & \\ \bullet & - & \bullet \\ & \bullet & \end{smallmatrix} \right\},$

(ii) $\mathcal{F}([4,4]) = R \left\{ \begin{smallmatrix} & \bullet & \\ \bullet & + & + \\ & \bullet & \end{smallmatrix} \,, \begin{smallmatrix} & \bullet & \\ \bullet & - & - \\ & \bullet & \end{smallmatrix} \right\},$

$$(iii) \quad \mathcal{F}([3,3]) = R\left\{ \begin{matrix} & + & \\ + & + & \bullet \\ & \bullet & \end{matrix} \ , \ \begin{matrix} & + & \\ \bullet & + & \bullet \\ & + & \end{matrix} \ , \ \begin{matrix} & - & \\ - & - & \bullet \\ & \bullet & \end{matrix} \ , \ \begin{matrix} & - & \\ \bullet & - & \bullet \\ & - & \end{matrix} \right\},$$

$$(iv) \quad \mathcal{F}([3,2]) = R\left\{ \begin{matrix} & + & \\ + & + & \bullet \\ & \bullet & \end{matrix} \ , \ \begin{matrix} & + & \\ \bullet & + & \bullet \\ & + & \end{matrix} \ , \ \begin{matrix} & - & \\ - & - & - \\ & \bullet & \end{matrix} \right\},$$

$$(v) \quad \mathcal{F}([2,2]) = R\left\{ \begin{matrix} & + & \\ + & + & + \\ & \bullet & \end{matrix} \ , \ \begin{matrix} & - & \\ - & - & - \\ & \bullet & \end{matrix} \right\},$$

$$(vi) \quad \mathcal{F}([1,1]) = \left\{ \begin{matrix} & + & \\ + & + & + \\ & + & \end{matrix} \ , \ \begin{matrix} & - & \\ - & - & - \\ & - & \end{matrix} \right\},$$

$$(vii) \quad \mathcal{F}([1,0]) = \left\{ \begin{matrix} & + & \\ + & + & + \\ & + & \end{matrix} \right\},$$

$$(viii) \quad \mathcal{F}([0,0]) = \phi.$$

Note that $\mathcal{F}([3,2])$ is not symmetric with respect to $+$ and $-$. This is a general phenomenon for $[m,n]$ whenever $m \neq n$. From (viii), we see that no mosaic pattern can be formed in region $[0,0]$.

We can glue two BP's together if they follow the rule given in Lemma 4.1. However, to construct all global mosaic patterns for each $[m,n]$, we need to find a more efficient way to glue appropriate feasible patterns together than using BP alone. To this end, we introduce the concept of building blocks and compatibility conditions for patching them together.

DEFINITION 4.6. *Let $\mathcal{P} \subset \mathcal{P}_3$ be a set of parameters in $\mathcal{P}_3$. $\mathcal{B} = \mathcal{B}(\mathcal{P})$, a (finite or infinite) set of feasible local patterns, is called a set of building blocks provided that every global mosaic pattern in $\mathcal{M}(\mathcal{P})$ can be generated by patching these building blocks together with respect to some compatibility condition $\mathcal{C}(\mathcal{P})$.*

If $\mathcal{P} = [m,n]$, we write $\mathcal{B}(\mathcal{P})$ as $\mathcal{B}([m,n])$, and $\mathcal{C}(\mathcal{P})$ as $\mathcal{C}([m,n])$. Note that for a given $\mathcal{P}, \{\mathcal{B}(\mathcal{P}), \mathcal{C}(\mathcal{P})\}$ is not necessarily unique if it does exist. However, we would like to have $\{\mathcal{B}(\mathcal{P}), \mathcal{C}(\mathcal{P})\}$ be such that as few elements as possible are in $\mathcal{B}(\mathcal{P})$, and rule $\mathcal{C}(\mathcal{P})$ is as simple as possible, since they are related to the transition matrices used to compute spatial entropy (see [39]) of $\mathcal{M}(\mathcal{P})$. Sometimes, a natural and obvious way can be used to find $\{\mathcal{B}(\mathcal{P}), \mathcal{C}(\mathcal{P})\}$ for certain $\mathcal{P}$. To find an efficient and effective $\{\mathcal{B}(\mathcal{P}), \mathcal{C}(\mathcal{P})\}$ for computing the entropy $h(\mathcal{M}(\mathcal{P}))$ we need the following definition.

DEFINITION 4.7. *Let $y_j : T_j \to \{-1, 1\}, j = 1, 2$, be two feasible local patterns with $T_1 \cap T_2 \neq \phi$. y_1 and y_2 then are called compatible if*

$$y_1 = y_2 \quad on \quad T_1 \cap T_2.$$

We say two feasible local patterns $y_j : T_j \to \{-1, 1\}, j = 1, 2$, are adjacent to another if $T_1 \cap T_2 = \phi$ and at least one cell from each set $T_j, j = 1, 2$, is adjacent to another.

We give the following simple compatibility rules to generate larger local patterns:

$\mathcal{C}_0$: Put together any two feasible local patterns y_1 and y_2 in $\mathcal{B}(\mathcal{P})$ that are adjacent to each other.

$\mathcal{C}_1$: Glue together any two feasible local patterns y_1 and y_2 in $\mathcal{B}(\mathcal{P})$ that are compatible.

Note that the feasibility $y_1 \cup y_2$ of both cases has to be verified. In practice, it is easy to check this by using BP in $\mathcal{F}([m,n])$. We begin with the study of symmetric region $[m,m]$ and then proceed with the asymmetric region $[m,n]$ for which $m \neq n$. We need to introduce additional notation.

DEFINITION 4.8.

(i) $H_k^+(H_k^-)$: a $+(-)$ pattern on horizontal infinite stripe H_k of width k in $\mathcal{Z}^2$.

(ii) $V_k^{\pm} = R(H_k^{\pm})$: a $+(-)$ pattern on vertical infinite stripe V_k of width k in $\mathcal{Z}^2$.

(iii) $H_k^{\times}$: a pattern having different signs in any adjacent cells on horizontal infinite stripe of width k.

(iv) $V_k^{\times} = R(H_k^{\times})$.

DEFINITION 4.9. An edge E_k of length k is a set consisting of k-many consecutive cells arranged horizontally or vertically, e.g., $\{(1,0),\ldots,(k,0)\}$ or $\{(0,1),\ldots,(0,k)\}$, and their translations in $\mathcal{Z}^2$. A solid edge $\tilde{E}_k$ in $\mathcal{R}^2$ of E_k is defined by $\tilde{E}_k = \{(x,0) : x \in \mathcal{R} \text{ and } 1 \leq x \leq k\}$ when $E_k = \{(1,0),\ldots,(k,0)\}$. Cells at both ends of E_k are called vertices. A path T is a disjoint union of (finitely or infinitely many) edges. A path T is called connected if its solid path $\tilde{T}$ is connected in $\mathcal{R}^2$. A nonempty subset T of $\mathcal{Z}^2$ is called a simple closed loop (or simple loop for short) if T is connected and satisfies

$$\#(N^+(i,j) \cap T) = 2$$

for each $(i,j) \in T$. A (simple) loop pattern y is a pattern defined on a simple loop T in $\mathcal{Z}^2$. A simple loop pattern is called finite (resp., infinite) if $\#(T) < \infty$ (resp., $\#(T) = \infty$). Let T be a finite simple closed loop, and $\tilde{T}$ be its solid path. The interior of T is the vertices inside $\tilde{T}$.

Remark 4.10.

(i) If T is a simple loop, then $\#(T)$ could be either finite or infinite. If $\#(T) < \infty$, then T must be closed in the following sense: starting and ending at the same vertex, every edge is traversed only once. If $\#(T) = 0$, we also say that T is a simple loop.

(ii) Since our template A is a square cross, the edges being considered are always horizontal or vertical. When $A = A^{\times}$, the diagonal cross, then the edges are diagonals in $\mathcal{Z}^2$. In this case, everything must be worked in the $N^{\times}$ sense.

We now give a list of building blocks for symmetric regions along with their construction rules.

THEOREM 4.11.

(I) For $[5,5]$, $\mathcal{B}([5,5]) = \{+,-\}$ and $\mathcal{C}([5,5]) = \mathcal{C}_0$.

(II) For $[4,4]$,

(i) if $a\varepsilon > 0$, $\mathcal{B}([4,4]) = R\{++,--\}$, and $\mathcal{C}([4,4]) = \mathcal{C}_0 \cup \mathcal{C}_1$.

(ii) if $a\varepsilon < 0$, $\mathcal{B}([4,4]) = R\{+-\}$, and $\mathcal{C}([4,4]) = \mathcal{C}_0 \cup \mathcal{C}_1$.

(III) For $[3,3]$,

(i) if $a\varepsilon > 0$, then $\mathcal{B}([3,3]) = \{$infinite simple patterns with the same signs$\} \cup \{$finite simple patterns with the same signs whose interiors are simple closed loops$\}$, and $\mathcal{C}([3,3]) = \mathcal{C}_0 \cup \mathcal{C}_1$.

(ii) if $a\varepsilon < 0$, then $\mathcal{B}([3,3])$ is the same as above except that adjacent saturated cells in simple patterns have different signs, and $\mathcal{C}([3,3]) = \mathcal{C}_0 \cup \mathcal{C}_1$.

(IV) For $[2,2]$,

(i) if $a\varepsilon > 0$, $\mathcal{B}([2,2]) = R\{H_2^{\pm}\}$ and $\mathcal{C}([2,2]) = \mathcal{C}_0 \cup \mathcal{C}_1$.

(ii) if $a\varepsilon < 0$, $\mathcal{B}([2,2]) = \{H_2^{\times}, V_2^{\times}\}$ and $\mathcal{C}([2,2]) = \mathcal{C}_0 \cup \mathcal{C}_1$.

(V) For $[1,1]$,

(i) $a\varepsilon > 0$, $\mathcal{M}([1,1]) = \{x = 1, x = -1\}$,

(ii) $a\varepsilon < 0$, $\mathcal{M}([1,1]) = \{checkerboard\ type\}$.

Proof. We only give the proof of (III (i)). The others are similar. Let $\mathcal{B}([3,3])$ and $\mathcal{C}([3,3])$ be as claimed in (III (i)). Denote by $\mathcal{M}(\mathcal{B}([3,3]), \mathcal{C}([3,3])$ the set of all patterns generated by the building blocks $\mathcal{B}([3,3])$ and compatibility rules $\mathcal{C}([3,3])$. To complete the proof of (III (i)), it then suffices to show that

$$\mathcal{M}(\mathcal{B}([3,3]), \mathcal{C}([3,3])) = \mathcal{M}([3,3]).$$

Clearly, $\mathcal{M}(\mathcal{B}([3,3]), \mathcal{C}([3,3])) \subset \mathcal{M}([3,3])$. Given $y = (y_{i,j}) = (f(x_{i,j})) \in \mathcal{M}([3,3])$, let Γ_+, and Γ_- be as defined in (2.2). Then, for each $(i,j) \in \Gamma_\bullet, \bullet = +$ or $-$, define

$T_{(i,j)}^\bullet = \{(p,q) \in \Gamma_\bullet$: there is a path of edges from (i,j) to (p,q) for which the states of all cells along the path have the same sign$\}$.

Since $y \in \mathcal{M}([3,3])$, we have that $\#(N^+(p,q) \cap T^\bullet(i,j)) = 2$ whenever $(p,q) \in T_{(i,j)}^\bullet, \bullet = +$ or $-$. Clearly, $T_{(i,j)}^\bullet, \bullet = +$ or $-$, is a simple closed loop. Moreover, $\cup_{(i,j)\in\Gamma_\bullet} T_{(i,j)}^\bullet = \Gamma_\bullet$, $\bullet = +$ or $-$. Note that the smallest positively sized finite simple closed loop must be of the form

$$
\begin{array}{cccccc}
+ & + & & - & - \\
+ & + & , & - & - .
\end{array}
$$

We shall call such a simple closed loop a rectangle of size 2×2. Therefore, if $T_{(i,j)}^+$ is a finite simple closed loop whose interior consists of $T_{(p,q)}^-$, for some $(p,q) \in \Gamma_-$, then the interior of $T_{(i,j)}^+$ must be the union of rectangles of size $m \times n$, where $m, n \geq 2$. Clearly, $y_{\Gamma_\bullet}$, $\bullet = +$, or $-$, is then formed by applying rules $\mathcal{C}_0$ and $\mathcal{C}_1$ to glue the building blocks together as given in (III (i)). $\square$

Now, we come to the asymmetric regions. It is clear that $[m,n]$ and $[n,m]$ give similar results if we just exchange the roles of $+$ and $-$. It is also easy to see that the patterns for $[m,1], m \geq 2$, are extremely simple. Indeed, the result of Theorem 4.11 (V) holds for these cases. Therefore, we need only study the cases of $[m,n]$ in which $2 \leq n < m \leq 5$. Comparing this with the result for $[3,3]$, we can easily obtain the following result for $[m,n]$ when $n \geq 3$.

THEOREM 4.12. *For $a\varepsilon > 0$, let $\mathcal{C} = \mathcal{C}_0 \cup \mathcal{C}_1$, and we have*

(I) $\mathcal{B}([5,4]) = R\{+, --\}$.

(II) $\mathcal{B}([5,3]) = \{+\} \cup \{simple\ loop\ patterns\ with\ negative\ signs\}$.

(III) $\mathcal{B}([4,3]) = \{++, \begin{smallmatrix} + \\ + \end{smallmatrix}\} \cup \{simple\ loop\ patterns\ with\ negative\ signs\ defined$

on a simple closed loop whose interior must consist of at least two cells$\}$.

The proof is similar to that used in proving the case of $[3,3]$ and is therefore omitted.

To generate mosaic patterns for $[m,2]$ and $[2,m], m \in I[3,5]$ and $a\varepsilon > 0$, we first note the following geometrical property of a feasible pattern.

LEMMA 4.13. *For the region $[m,2], m \geq 3$, and $a\varepsilon > 0$, let T be a rectangle in $\mathcal{Z}^2$ and $T_1 \subset T$ such that $T_1 \cap \partial T = \phi$, where ∂T is the boundary of T. Assume that $y : T \to \{-1, 1\}$ is a feasible pattern with respect to $[m,2]$ and satisfies*

$$y_{i,j} = 1 \quad in \quad T_1,$$
$$and\ y_{i,j} = -1 \quad on \quad \partial T.$$

Then T_1 has to be a rectangle.

The idea behind the proof of Lemma 4.13 is that no negatively saturated cell can be placed at any corner in $\mathcal{Z}^2$ that is adjacent to two positively saturated cells. Therefore, T_1 must be a rectangle. Details of the proof are omitted. With Lemma 4.13 in mind, we can induce more building blocks and define compatibility conditions for $[m, 2]$ and $[2, m], m \in I[3, 5]$ and $a\varepsilon > 0$.

Let $t = (\ldots s_{-1}, s_0, s_1, s_2, \ldots)$ be a two-sided sequence. Here, $s_i \in \mathbf{N} \cup \{\infty\} - \{1\}$. Moreover, if $s_i = \infty$, and $s_{i-1} \neq \infty$, then $t = (\ldots, s_{-1}, s_0, s_1, \ldots s_i)$. If $s_i = \infty$, and $s_{i+1} \neq \infty$, then $t = (s_i, s_{i+1}, \ldots)$. If $s_i = s_k = \infty$, $i < k$, then $t = (s_i, s_{i+1}, \ldots, s_k)$. The set of all such sequences is denoted by Σ. We also denote by $S^+(t)$ the $+$ pattern on an alternative array of vertical upper- and lower-half infinite stripes whose corresponding widths are prescribed by a (two-sided) sequence t. An example of $S^+(t)$ in which $t = (s_{-2}, s_{-1}, s_0, s_1, s_2) = (\infty, 3, 4, 5, \infty)$ is given below.
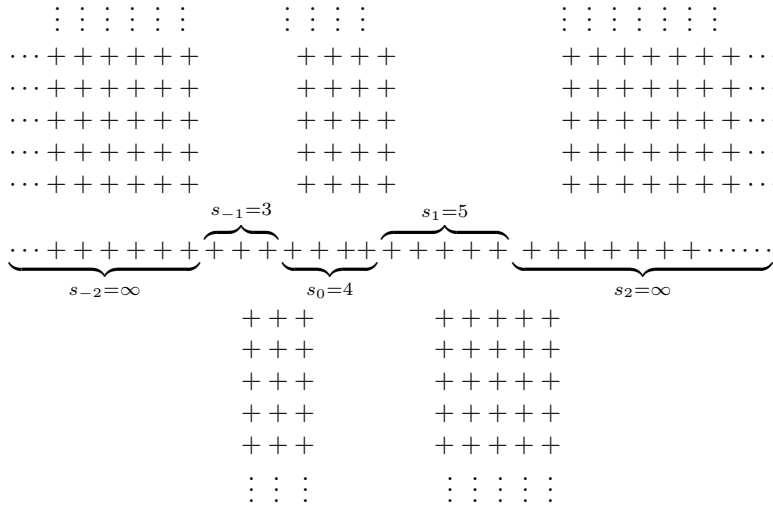
We define $S^-(t)$ in similar fashion.

We also define the following compatibility condition.

$\mathcal{C}_k(-, m)$(resp., $\mathcal{C}_k(+, m)$), $k = 0$ or 1, and $m \in I[3, 5]$:

> To generate a global mosaic pattern in $[m, 2]$ (resp., $[2, m]$), the compatibility rule $\mathcal{C}_k(-, m)$ is first applied to feasible local patterns that have negative (resp., positive) signs. Once the patching of these feasible local patterns is done (after finitely or infinitely many times), the unfilled space, which is to be filled with positive (resp., negative) signs, must be a rectangle of at least size $k \times \ell$, where $k, \ell \in \mathbf{N} \cup \{\infty\}$, and $\max\{k, \ell\} \geq (5-m)$, for 4 or 5, and $\min\{k, \ell\} \geq 2$ for $m = 3$. We then use $\mathcal{C}_k$ to fill in those unfilled spaces with feasible local patterns that have positive (resp., negative) signs.

We are now ready to state the following results. The proof is similar to that used in proving Theorem 4.11 and is omitted here.

THEOREM 4.14. *For $a\varepsilon > 0$, we have*

(I) $\mathcal{B}([5, 2]) = \{+\} \cup \{H_2^-, V_2^-\} \cup R\{S^-(t) : t \in \Sigma\}$.
  $\mathcal{C}([5, 2]) = \mathcal{C}_0(-, 5) \cup \mathcal{C}_1(-, 5)$.

(II) $\mathcal{B}([4,2]) = \{++, \begin{smallmatrix} + \\ + \end{smallmatrix}, H_2^-, V_2^-\} \cup R\{S^-(t) : t \in \Sigma\}.$

$\mathcal{C}([4,2]) = \mathcal{C}_0(-, 4) \cup \mathcal{C}(-, 4).$

(III) $\mathcal{B}([3,2]) = \{\begin{smallmatrix} + & + \\ + & + \end{smallmatrix}, H_2^-, V_2^-\} \cup R\{S^-(t) : t \in \Sigma\}.$

$\mathcal{C}([3,2]) = \mathcal{C}_0(-, 3) \cup \mathcal{C}_1(-, 3).$

(IV) *Define* $-\mathcal{B}([5,2]) = \{-\} \cup \{H_2^+, V_2^+\} \cup R\{S^+(t) : t \in \Sigma\}.$

Here, we interchange "+" with "−". Define $-\mathcal{B}([m,2])$ *and* $-\mathcal{C}([m,2])$, $m \in I[3,5]$, *similarly. Then, for* $m \in I[3,5]$,

$$\mathcal{B}([2,m]) = -\mathcal{B}([m,2]),$$
$$\mathcal{C}([2,m)) = -\mathcal{C}([m,2]).$$

Based on the results from Theorems 4.11 and 4.14, we can compute the lower bounds of the spatial entropy of $\mathcal{M}([m,n])$, the set of all mosaic patterns of $[m,n]$. We first prove the following theorem.

THEOREM 4.15. *Let* $m, n \in I[0,5]$, *and let*

(4.3) $$\alpha = \max\{m,n\} \quad \text{and} \quad \beta = \min\{m,n\}.$$

Equation (2.1) *then exhibits spatial chaos if and only if* $\alpha \geq 3$ *and* $\beta \geq 2$.

Proof. It is clear $\mathcal{M}([m,n])$ is monotonous with respect to m and n, e.g., if $m_1 \leq m_2$ and $n_1 \leq n_2$, then

$$\mathcal{M}([m_1, n_1]) \subseteq \mathcal{M}([m_2, n_2]).$$

To prove the theorem, it suffices to show only that

(4.4) $$h(\mathcal{M}([2,2])) = 0$$

and

(4.5) $$h(\mathcal{M}([3,2])) > 0.$$

We first prove (4.4). Let $N = (N_1, 2)$ and $N_1 \geq 2$. We then have

$$\Gamma_N(\mathcal{M}([2,2])) \leq 4.$$

Hence, (4.4) holds. To prove (4.5), we may assume $a\varepsilon > 0$, the case in which $a\varepsilon < 0$ can be treated analogously. Consider a rectangle of size $4n_1 \times 4n_2$ in $\mathcal{Z}^2$. So, there are $n_1 \cdot n_2$ many squares of size 4×4.

Consider the following choices of patterns for a 4×4 square:

(4.6)
$$
\begin{matrix}
- & - & - & - \\
- & - & - & - \\
+ & + & - & - \\
+ & + & - & -
\end{matrix}
\qquad
\begin{matrix}
- & - & - & - \\
- & - & - & - \\
- & - & - & - \\
- & - & - & -
\end{matrix}
\ .
$$

They are feasible and compatible with each other in $[3,2]$. Therefore, they can be glued together at random. Hence, for $N = (4n_1, 4n_2)$, we have

(4.7) $$\Gamma_N(\mathcal{M}([3,2])) \geq 2^{n_1 n_2}.$$

From (4.7), it is not difficult to prove that

$$(4.8) \qquad h(\mathcal{M}([3,2])) \geq \frac{log\,2}{16}.$$

The proof of the theorem is thus complete. □

Furthermore, we can obtain some lower bounds for $h(\mathcal{M}([m,n]))$. When (4.3) holds, some lower bounds for $h(M([m,n]))$ can be obtained by the following.

THEOREM 4.16.

$$(4.9) \qquad h(\mathcal{M}([m,n])) \geq \begin{cases} log\,2 & if \ \beta = 5, \\[2mm] \frac{log\,10}{4} & if \ \beta = 4, \\[2mm] \frac{log\,4}{4} & if \ \beta = 3, \\[2mm] \frac{log\,4}{9} & if \ \beta = 2, \alpha = 5, \\[2mm] \frac{log\,4}{12} & if \ \beta = 2, \alpha = 4, \\[2mm] \frac{log\,2}{16} & if \ \beta = 2, \alpha = 3. \end{cases}$$

Proof. We give only a proof for $[5,4]_\varepsilon, a\varepsilon > 0$. The other cases can be treated similarly.

Consider a rectangle of size $2n_1 \times 2n_2$. Then each of the 2×2 squares can have any of the following choices:

$$\begin{matrix} ++ & +- & ++ & -+ & -- & +- & -+ & -- & -- & -- \\ ++, & +-, & --, & -+, & ++, & --, & --, & -+, & +-, & --. \end{matrix}$$

So,

$$\Gamma_N(\mathcal{M}(z,a;\varepsilon)) \geq 10^{n_1 n_2}.$$

Hence,

$$h(\mathcal{M}(z,a;\varepsilon)) \geq \frac{log10}{4}. \qquad □$$

Remark 4.17. All the results obtained here can be directly generalized to encompass the case in which template A is diagonally crossed. Moreover, the techniques used here are, in principle, applicable to the case in which template A is of the form given in (3.14).

5. One-dimensional CNNs. In this section, by using the same method used for two-dimensional CNNs, we briefly discuss the problems associated with one-dimensional CNNs. We consider a one-dimensional CNN described by the space-invariant symmetric A-template

$$(5.1) \qquad A = [a\varepsilon \ \ a \ \ a\varepsilon].$$

The equations describing this CNN are thus given by

$$(5.2) \qquad \frac{dx_i}{dt} = -x_i + z + a\varepsilon f(x_{i-1}) + af(x_i) + a\varepsilon f(x_{i+1}), i \in \mathcal{Z}.$$
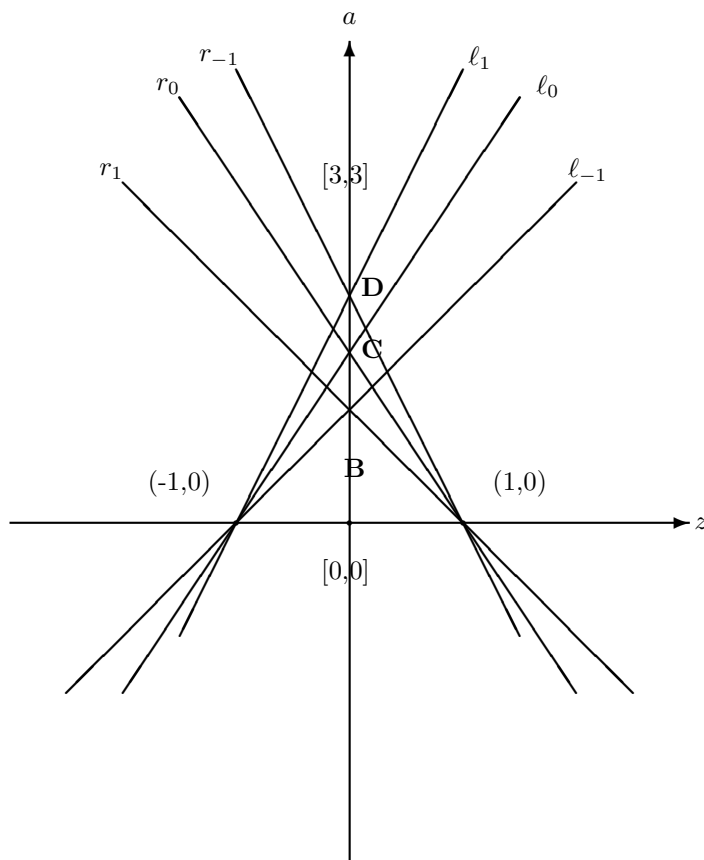
FIG. 5.1.

The stable defect solutions for $z = 0$ and their spatial entropy complexities were studied in [39]. We begin by stating the results for mosaic solutions.

Notation 5.1. Let $m, n \in I[0, 3]$. Given $\varepsilon \neq 0, \varepsilon \in R$, we denote as $[m, n]_\varepsilon$ the region on the $z - a$ plane in which the following restrictions hold:

(1) Any positively saturated cell is adjacent to at least $3 - m$ positively (resp., negatively) saturated cells, provided that $a\varepsilon > 0$ (resp., $a\varepsilon < 0$).

(2) Any negatively saturated cell is adjacent to at least $3 - n$ negatively (resp., positively) saturated cells, provided that $a\varepsilon > 0$ (resp., $a\varepsilon < 0$).

For $m = 3$, this means that any positively saturated cell can be adjacent to either a positively or negatively saturated cell. For $m = 0$, this means that no positively saturated cell ever exists in a pattern. For $n = 3$ or $n = 0$, the interpretations are similar. We next give a complete classification for mosaic solutions in the $(z, a; \varepsilon)$ parameter space, which is decomposed in terms of $[m, n]_\varepsilon$ regions.

THEOREM 5.2.

(i) *For $0 < |\varepsilon| < \frac{1}{2}$, the $z - a$ plane is decomposed, in terms of $[m, n]_\varepsilon$ regions, as follows:*

Here $\ell_i = \ell_{i,\varepsilon}$ and $r_i = r_{i,\varepsilon}$, $i \in I[-1, 1]$, are given in (3.5) and (3.6). The regions $[m, n]_\varepsilon$, $m, n \in I[0, 3]$, in Figure 5.1 are located similarly to those in Figure 3.4.
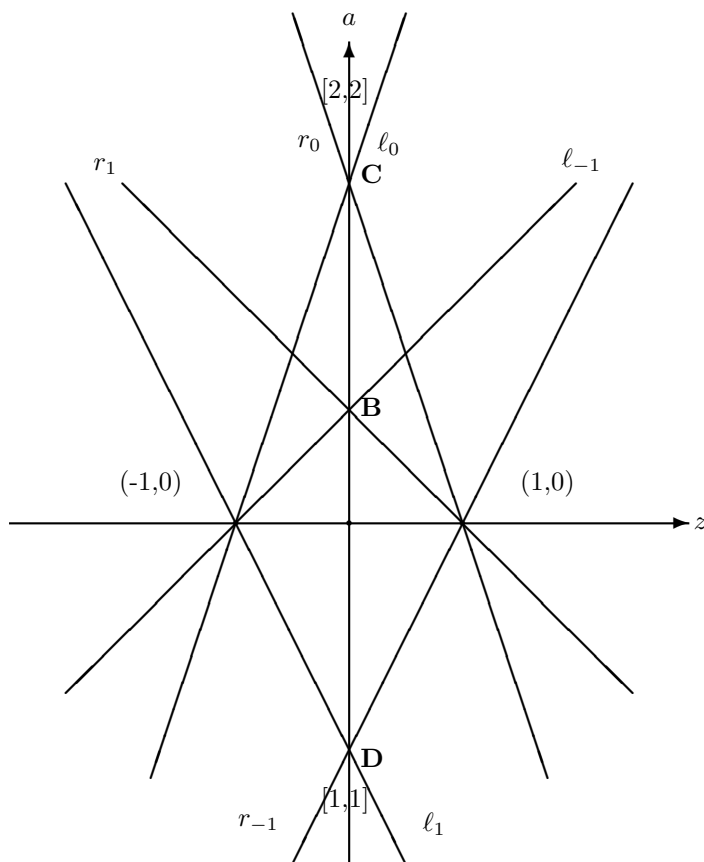
FIG. 5.2.

(ii) *For $|\varepsilon| \geq \frac{1}{2}$, the $z - a$ plane is decomposed into $[m, n]_\varepsilon$ regions, as shown in Figure 5.2.*

Region $[3, 3]_\varepsilon$ no longer exists for $|\varepsilon| \geq \frac{1}{2}$. For $\varepsilon \geq 1$, regions $[3, 2]_\varepsilon$ and $[2, 3]_\varepsilon$ also disappear. Moreover, for $\varepsilon > 1$, a new piece of each of the regions $[2, 1]_\varepsilon$ and $[1, 2]_\varepsilon$ will appear on the lower half of the $z - a$ plane.

Unlike a two-dimensional CNN, the complexity of the mosaic patterns can be computed exactly using a transition matrix; the results are summarized as follows.

THEOREM 5.3. *Suppose $(z, a) \in [m, n]_\varepsilon, \varepsilon \neq 0$. Then system (5.1) exhibits spatial chaos if and only if $\min\{m, n\} \geq 2$. Moreover,*

$$h(\mathcal{M}(z, a; \varepsilon)) = \begin{cases} ln2 & if \quad m = n = 3, \\ ln\lambda & if \quad m = 2 \quad and \quad n = 3 \quad or \quad m = 3 \quad and \quad n = 2, \\ ln\dfrac{1 + \sqrt{5}}{2} & if \quad m = n = 2. \end{cases}$$

Here λ is the maximal root of $\lambda^3 - 2\lambda^2 + \lambda - 1 = 0$.

Proof. We give a proof only for the spatial entropy of regions $[2, 2]_\varepsilon$ and $[3, 2]_\varepsilon, a\varepsilon > 0$. Let $(z, a) \in [2, 2]_\varepsilon, a\varepsilon > 0$. Then, $++$ and $--$ are building blocks. If 1 is identified as the positively saturated cell whose right-hand neighbor is also a positively

saturated cell, and 2 as the positively saturated cell whose right-hand neighbor is a negatively saturated cell, in notation we have

$$\oplus+ \leftrightarrow 1,$$

$$\oplus- \leftrightarrow 2.$$

Similarly, we assign $\ominus-$ and $\ominus+$ to 3 and 4. The transition matrix for this type of patterns is then

$$A_1 = \begin{bmatrix} 1 & 1 & 0 & 0 \\ 0 & 0 & 1 & 0 \\ 0 & 0 & 1 & 1 \\ 1 & 0 & 0 & 0 \end{bmatrix}.$$

Clearly, the maximal eigenvalue for A_1 is $\frac{1+\sqrt{5}}{2}$. Suppose $(z,a) \in [2,3]_\varepsilon, a\varepsilon > 0$. Then $++$ and $-$ are building blocks and we have the following identification:

$$\oplus+ \leftrightarrow 1,$$

$$\oplus- \leftrightarrow 2,$$

$$- \leftrightarrow 3,$$

and the corresponding matrix is

$$A_2 = \begin{bmatrix} 1 & 1 & 0 \\ 0 & 0 & 1 \\ 1 & 0 & 1 \end{bmatrix}.$$

The characteristic polynomial for A_2 is

$$\lambda^3 - 2\lambda^2 + \lambda - 1 = 0.$$

For brevity, we skip the remainder of the proof. □

Remark 5.4. (i) Note that $\frac{1+\sqrt{5}}{2} < \lambda < 2$. (ii) All mosaic solutions are stable as in the two-dimensional case.

6. Conclusion. This paper investigated properties of mosaic pattern in cellular neural networks with a bias term z, and a symmetric and square-crossed template A.

In the one- and two-dimensional cases, a complete characterization of the stable mosaic patterns has been obtained, together with a measure of their number and complexity. In particular, for given $\varepsilon \neq 0$, (z,a)-plane is decomposed into mutually disjoint regions $[m,n]_\varepsilon$, $m,n \in I[0,5]$. Moreover, as numbers m and n increase, or equivalently, the parameter a moves north, the complexity of the patterns increases. We found that if $\max\{m,n\} \geq 3$ and $\min\{m,n\} \geq 2$, then the system exhibits chaos; otherwise, it has pattern formation. All stationary patterns obtained by numerical computations [11, 12, 13, 15, 16, 19, 33, 36, 39, 41] are consistent with our theoretical results.

REFERENCES

[1] V. S. Afraimovich and V. I. Nekorkin, *Chaos of traveling waves in a discrete chain of diffusively coupled maps*, Internat. J. Bifur. Chaos Appl. Sci. Engrg., 4 (1994), pp. 631–637.

[2] V. S. Afraimovich and Y. G. Pesin, *Traveling waves in lattice models of multi-dimensional and multi-component media*, I. *General hyperbolic properties*, Nonlinearity, 6 (1993), pp. 429–455; II. *Ergodic properties and dimension*, Chaos, 3 (1993), pp. 233–241.

[3] J. Bell, *Some threshold results for modes of myelinated nerves*, Math. Biosci., 54 (1981), pp. 181–190.

[4] J. Bell and C. Cosner, *Threshold behavior and propagation for nonlinear differential-difference systems motivated by modeling myelinated axons*, Quart. Appl. Math., 42 (1984), pp. 1–14.

[5] J. W. Cahn, *Theory of crystal growth and interface motion in crystalline materials*, Acta Metallurgica, 8 (1960), pp. 554–562.

[6] J. W. Cahn, J. Mallet-Paret, and E. S. Van Vleck, *Traveling wave solutions for systems of ODEs on a two-dimensional spatial lattice*, SIAM J. Appl. Math., 59 (1998), pp. 455–493.

[7] S. N. Chow and J. Mallet-Paret, *Pattern formation and spatial chaos in lattice dynamical system*, IEEE Trans. Circuits Systems I Fund. Theory Appl., 42 (1995), pp. 746–751.

[8] S. N. Chow, J. Mallet-Paret, and E. S. Van Vleck, *Pattern formation and spatial chaos in spatially discrete evolution equations*, Random Comput. Dynam., 4 (1996), pp. 109–178.

[9] S. N. Chow, J. Mallet-Paret, and E. S. Van Vleck, *Dynamics of lattice differential equations*, Internat. J. Bifur. Chaos Appl. Sci. Engrg., 9 (1996), pp. 1605–1621.

[10] S. N. Chow and W. Shen, *Stability and bifurcation of traveling wave solutions in coupled map lattices*, J. Dynam. Systems Appl., 4 (1995), pp. 1–26.

[11] L. O. Chua and T. Roska, *The CNN paradigm*, IEEE Trans. Circuits Systems, 40 (1993), pp. 147–156.

[12] L. O. Chua and L. Yang, *Cellular neural networks: Theory*, IEEE Trans. Circuits Systems, 35 (1988), pp. 1257–1272.

[13] L. O. Chua and L. Yang, *Cellular neural networks: Applications*, IEEE Trans. Circuits Systems, 35 (1988), pp. 1273–1290.

[14] H. E. Cook, D. de Fontaine, and J. E. Hilliard, *A model for diffusion on cubic lattices and its application to the early stages of ordering*, Acta Metallurgica, 17 (1969), pp. 765–773.

[15] K. R. Crounse and L. O. Chua, *Methods for image processing and pattern formation in cellular neural networks*, IEEE Trans. Circuits Systems I Fund. Theory Appl., 42 (1995), pp. 583–601.

[16] K. R. Crounse, L. O. Chua, P. Thiran, and G. Setti, *Characterization and dynamics of pattern formation in cellular neural networks*, Internat. J. Bifur. Chaos Appl. Sci. Engrg., 6 (1996), pp. 1703–1724.

[17] G. B. Ermentrout, *Stable periodic solutions to discrete and continuum arrays of weakly coupled nonlinear oscillators*, SIAM J. Appl. Math., 52 (1992), pp. 1665–1687.

[18] G. B. Ermentrout and N. Kopell, *Inhibition-produced patterning in chains of coupled nonlinear oscillators*, SIAM J. Appl. Math., 54 (1994), pp. 478–507.

[19] T. Erneux and G. Nicolis, *Propagating waves in discrete bistable reaction-diffusion systems*, Phys. D, 67 (1993), pp. 237–244.

[20] W. J. Firth, *Optical memory and spatial chaos*, Phys. Rev. Lett., 61 (1988), pp. 329–332.

[21] M. Haenggi, *Java CNN Simulator*, http://www.isi.ee.ethz.ch/∼haenggi/CNNsim.html.

[22] M. Hillert, *A solid-solution model for inhomogeneous systems*, Acta Metallurgica, 9 (1961), pp. 525–535.

[23] C. H. Hsu and S. S. Lin, *Spatial Disorder of Cellular Neural Networks*, preprint.

[24] C. H. Hsu and S. S. Lin, *Travelling waves in lattice dynamical system with applications to cellular neural networks*, J. Differential Equations, to appear.

[25] C. H. Hsu, J. Juang, S. S. Lin, and W. W. Lin, *Cellular neural networks: Local patterns for general templates*, Internat. J. Bifur. Chaos, to appear.

[26] J. Juang and S. S. Lin, *Cellular Neural Networks: Defect Pattern and Spatial Chaos*, preprint.

[27] J. P. Keener, *Propagation and its failure in coupled systems of discrete excitable cells*, SIAM J. Appl. Math., 47 (1987), pp. 556–572.

[28] J. P. Keener, *The effects of discrete gap junction coupling on propagation in myocardium*, J. Theor. Biol., 148 (1991), pp. 49–82.

[29] J. P. Laplante and T. Eveneux, *Propagation failure in arrays of coupled bistable chemical reactors*, J. Phys. Chem., 96 (1992), pp. 4931–4934.

[30] N. Kopell, G. B. Ermentrout, and T. L. Williams, *On chains of oscillators forced at one end*, SIAM J. Appl. Math., 51 (1991), pp. 1397–1417.

[31] R. S. MacKay and J. A. Sepulchre, *Multistability in networks of weakly coupled bistable units*, Phys. D, 82 (1995), pp. 243–254.

[32] J. Mallet-Paret, *Spatial patterns, spatial chaos, and traveling waves in lattice differential equations*, in Akademie Colloquium, Dynamical Systems and their Applications, Amsterdam, 1995, Koninklijke Nederlandse Akademic van Wetenschappen Verhandelingen, Afd. Natuurkunde, Eerste Reeks, S. J. van Strien and S. M. Verduyn Lunel, eds., North-Holland, Amsterdam, 1996, pp. 105–129.

[33] J. Mallet-Paret and S. N. Chow, *Pattern formation and spatial chaos in lattice dynamical systems*, II, IEEE Trans. Circuits Systems, 42 (1995), pp. 752–756.

[34] A. Perez-Munuzuri, V. Perez-Munuzuri, V. Perez-Villar, and L. O. Chua, *Spiral waves on a 2-d array of nonlinear circuits*, IEEE Trans. Circuits Systems, 40 (1993), pp. 872–877.

[35] C. Robinson, *Dynamical Systems*, CRC Press, Boca Raton, FL, 1995.

[36] T. Roska, L. O. Chua, D. Wolf, T. Kozek, R. Tetzlatf, and F. Puffer, *Simulating nonlinear waves and partial differential equations via CNN, Part* I*: Basic techniques*, IEEE Trans Circuits Systems, 42 (1995), pp. 807–815.

[37] C. W. Shih, *Pattern formation and spatial chaos for cellular neural networks with asymmetric templates*, Internat. J Bifur. Chaos Appl. Sci. Engrg., 8 (1998), pp. 1907–1936.

[38] C.-W. Shih, *Influence of boundary conditions on pattern formation and spatial chaos in lattice systems*, SIAM J. Appl. Math., to appear.

[39] P. Thiran, K. R. Crounse, L. O. Chua, and M. Hasler, *Pattern formation properties of autonomous cellular neural networks*, IEEE Trans. Circuits Systems, 42 (1995), pp. 757–774.

[40] R. L. Winslow, A. L. Kimball, and A. Varghese, *Simulating cardiac sinus and atrial network dynamics on the connection machine*, Phys. D, 64 (1993), pp. 281–298.

[41] *Special issue on nonlinear waves, patterns and spatio-temporal chaos in dynamic arrays*, IEEE Trans. Circuits Systems I Fund. Theory Appl., 42 (October 1995).